DOCTOR OF SCIENCES

Study of the mode of action of COS-OGA, a new class of elicitors of plant innate immunity

van Aubel, Géraldine

Award date:
2017

Awarding institution:
University of Namur

CHAPTER 3

Plant immunity induced by COS-OGA elicitor is a cumulative process that involves salicylic acid

Géraldine van Aubel[1], Pierre Cambier[1], Marc Dieu[2], and Pierre Van Cutsem[1]

Published in Plant Science 247 (2016) 60-70, available online

[1] Research Unit in Plant Cellular and Molecular Biology, Namur University, Namur, Belgium

[2] Laboratory of Cellular Biochemistry and Biology, University of Namur, Belgium

Abstract

Plant innate immunity offers considerable opportunities for plant protection but beside flagellin and chitin, not many molecules and their receptors have been extensively characterized and very few have successfully reached the field. COS-OGA, an elicitor that combines cationic chitosan oligomers (COS) with anionic pectin oligomers (OGA), efficiently protected tomato (*Solanum lycopersicum*) grown in greenhouse against powdery mildew (*Leveillula taurica*). Leaf proteomic analysis of plants sprayed with COS-OGA showed accumulation of Pathogenesis-Related proteins (PR), especially subtilisin-like proteases. qRT-PCR confirmed upregulation of PR-proteins and salicylic acid (SA)-related genes while expression of jasmonic acid/ethylene-associated genes was not modified. SA concentration and class III peroxidase activity were increased in leaves and appeared to be a cumulative process dependent on the number of sprayings with the elicitor. These results suggest a systemic acquired resistance (SAR) mechanism of action of the COS-OGA elicitor and highlight the importance of repeated applications to ensure efficient protection against disease.

1. Introduction

Beside structural barriers and constitutive secondary metabolites, plants permanently monitor their environnement and have the capacity to detect microorganisms. The sentinels of the plant immunity are pattern recognition receptors (PRRs) which are receptor kinases essentially localized to the plasma-membrane and able to detect conserved molecular patterns often called elicitors. These molecules comprise both non-self conserved microbial signatures (pathogen-associated molecular patterns, PAMPs) and self molecules (damage-associated molecular patterns, DAMPs). After perception at the cell level, changes in plant hormone levels, mainly salicylic acid (SA) and jasmonic acid (JA), allow a coordinated response of the whole plant against potential invaders (Pieterse *et al.*, 2012). These events collectively lead to the establishment of PAMP-triggered immunity (PTI) also called basal immunity or horizontal resistance (Boller and Felix, 2009). The plant answer must be adapted to the pathogen's feeding strategy, whether necrotrophy or biotrophy. With many exceptions, the current belief is that the SA pathway provides protection against biotrophic pathogens and some phloem-feeding insects and the JA pathway is linked to resistance against necrotrophic pathogens and chewing herbivores (Fu and Dong, 2013). Several crosstalks exist between these hormonal signaling pathways, the most characterised being between SA, JA and ethylene (ET) in *Arabidopsis*. The regulation is often based on chromatin modifications and transcription factors (Pieterse *et al.*, 2012). The crossroad between these hormones is the non expressor of PR genes 1 (NPR1) protein, recently characterized as a SA receptor (Kuai *et al.*, 2015). NPR1 is also involved in SA suppression of JA pathway as plants seem to prioritize SA over JA. But ET can adjust finely the prioritization of plant defense pathways. Indeed, when ET and JA are both present, plants become insensitive to SA supression of JA pathway and in presence of both SA and ET, NPR1 is not anymore required for SA suppression of the JA pathway (Thaler *et al.*, 2012).

Reactive oxygen species (ROS) are important modulators of PTI, particularly apoplastic ROS produced in the early stages of biotic interactions by membrane-bound NADPH oxidases (RBOH) and cell wall-localized class III peroxidases (Daudi *et al.*, 2012). It was recently shown that upon elongation factor Tu and flagellin (flg22) recognition by their associated PRR, RBOHD is directly activated to ensure a rapid extracellular oxidative burst (Kadota *et al.*, 2014). ROS can be sensed through direct oxidative modificiations of lipids and proteins as well as modification of the cell redox status. Most of the time SA and JA

antagonism is potentiated by ET and mainly regulated by ROS and mitogen-activated protein kinases acting downstream of transcription factors including NPR1, JAZ and WRKYs (Pieterse *et al.*, 2012; Thaler *et al.*, 2012). Synergisitic effects have also been reported, especially after pathogen challenge when effective plant defense requires the three hormonal pathways (Sanchez *et al.*, 2012).

This article focuses on COS-OGA, an elicitor resulting from the association of both plant self and non-self molecules: pectin-derived oligogalacturonides (OGA) and chitooligosaccharides (COS), respectively. The combination mimics a plant-pathogen interaction when upon plant penetration, fungi deacetylate their wall chitin into chitosan to escape plant chitin receptors (El Gueddari *et al.*, 2002). Chitosan fragmentation by plant enzymes yields oligocationic COS molecules while plant cell wall degradation by fungal polygalacturonases releases polyanionic OGA molecules able to dimerize with calcium under the egg box conformation. COS interact with OGA egg boxes to form a stabilized complex called COS-OGA that triggers defense responses in *Arabidopsis thaliana* cell suspensions (Cabrera *et al.*, 2010). COS-OGA has been shown to efficiently protect grapevine and cucumber against powdery mildew (van Aubel *et al.*, 2014). The aim of this study is to shed some light into the molecular basis of plant protection conferred by this elicitor. Tomato plants, *Solanum lycopersicum* L. were treated with COS-OGA and a 2D-DIGE proteomic study was carried out and followed by qRT-PCR on specific defense-related genes to start decifering the signaling pathway triggered by this elicitor. Finally COS-OGA was tested against powdery mildew disease provoked by *Leveillula taurica* (Lev.) Arn. on tomato grown in greenhouse.

2. Methods

2.1. Biological material, growth conditions and treatments

Tomato plants (*S. lycopersicum*, CV Moneymaker) were grown on loam at 24°C with a 16 h/8 h day/night regime. Twenty-four hours before the first treatment, four week-old plants were transferred in a growth cabinet at 20°C, 90% relative humidity with a 16 h/8 h day/night regime. Elicitor was applied until run off with a hand sprayer on both sides of the leaves. Control plants were sprayed with 50 mM NaCl, 0.5 mM $CaCl_2$, 0.1% Dehscofix® CO 95 (Huntsman), pH 5 and COS-OGA-treated plants were sprayed with the same solution containing 50 ppm COS-OGA elicitor which is a combination of 25 ppm COS and 25 ppm

OGA prepared as described by Cabrera et *al.* (2010). For comparison, plants were also similarly sprayed with 0.1% Tween 20 or with 5 ppm flg22 (GenScript) with 0.1% Tween 20. Leaf samples were harvested 24 h after each treatment and cryogenically ground.

2.2. Peroxidase activity

Frozen leaf samples (0.5 g) were homogenized in 2 ml 50 mM ice-cold sodium acetate, 1 M NaCl, 5 mM EDTA, pH 5.2. After centrifugation at 17,000 g, the supernatant was collected and protein content was determined with Pierce 660 nm Protein Assay (Thermo Scientific). Guaiacol peroxidase activity measurement was followed at 420 nm for 5 min on crude protein extracts mixed with 0.2 M H_2O_2, 0.2 M guaiacol in 100 mM phosphate buffer, pH 5.8. Guaiacol peroxidase activity was then expressed as percentage of the control average value. Normalized peroxidase activities were analyzed using ANOVA and Student Newman Keuls (SNK) test for multiple comparisons ($P < 0.05$).

2.3. Extraction of total soluble proteins

Cryogenically-ground leaf samples (0.5 g) were homogenized in 10 mL precipitation buffer (acetone/TCA/2-mercaptoethanol, 89.9/10/0.1 v/v) and incubated for 1 h at -20°C. After centrifugation at 15,000 g, the protein pellet was washed three times with 10 mL washing buffer (acetone/2-mercaptoethanol, 99.9/0.1 v/v). A fourth and last wash was carried out overnight at -20°C. The protein pellets were dried under vacuum and solubilized in 7 M urea, 2 M thiourea, 4% CHAPS, 30 mM Tris, pH 8.5. Protein contents were assayed with Pierce 660 nm Protein Assay as described above.

2.4. 2D-DIGE on total soluble proteins

Four analytical gels corresponding to four biological replicates were prepared. Protein samples were labelled with cyanine fluorescent dyes (CyDye, Cy3, Cy2, Cy5, GE Healthcare). Cy2 was used as the internal standard which was composed of equal quantity of proteins of each replicates while Cy3 and Cy5 were used to label samples. Labelling of samples, rehydration of Immobiline Dry Strips, pI 4-7 (24 cm, GE Healthcare) and loading of protein samples followed by isoelectrical focusing on Ettan IPGphor II (GE Healthcare) was performed as previously described (Roland *et al.*, 2013). Strips were then loaded onto 10% polyacrylamide gels and the second dimension electrophoresis was launched on Ettan DALT six electrophoresis unit (GE Healthcare) at 15°C for 1 h at 3 W and 17 h at 6 W.

2.5. Image and data analysis for 2D-DIGE

After migration, analytical gels were scanned with a Typhoon 9400 imager (GE Healthcare) and analyzed with the DeCyder 2D Differential Analysis software 6.0 (GE Healthcare). Protein spots varying more than 1.2 fold between control and COS-OGA-treated plants were detected by Student's t-test with $P < 0.05$ for variation.

2.6. Spot picking, in-gel digestion and mass spectrometry

For protein identification, two preparative gels, each including 150 µg proteins of mixed samples were performed as described above but post-stained with krypton (Roland *et al.*, 2013). Differentially abundant protein spots selected on analytical gels were picked on preparative gels with Ettan Spot Picker (GE Healthcare). Trypsinized peptides from two preparative gels were pooled and analyzed with nano-LC-ESI-MS/MS maXis 4G UHR-TOF mass spectrometer (Bruker) coupled with a 2D-LC Dionex UltiMate 3000 (Thermo Scientific) as previously described (Pierrard *et al.*, 2012). The digests were separated by reverse-phase liquid chromatography using a 75 µm X 150 mm C18 Dionex column (Acclaim PepMap 100 C18) in an Ultimate 3000 liquid chromatography system (Dionex). The five most intense peptide ions 2+ or 3+ were sequenced. MaXis and Dionex systems were run under Compass HyStar 3.2 (Bruker). Tandem mass spectra were extracted, charge state deconvoluted and deisotoped by DataAnalysis version 4.0.

Peak lists were created using DataAnalysis 4.0 (Bruker) and saved as MGF files for use with ProteinScape 3.0 (Bruker) and Mascot 2.2 as search engine (Matrix Science). The protein database was downloaded on January 22, 2016 from Sol Genomics Network (ftp://ftp.solgenomics.net/proteomics/Solanum_lycopersicum/) containing 34,727 sequences. The following parameters were adopted for database searches: digestion by trypsin, peptide mass tolerance of 7 ppm, peptide fragments tolerance of 0.05 Da, maximum one missed cleavage, cysteine carbamidomethylation as a fixed modification, glutamine conversion to pyroglutamate on the N terminus, and methionine oxidation as variable modifications, a significance threshold of 0.05, a minimal peptide score of 30 with at least two peptides per protein with an identity score.

2.7. Measurement of gene expression by quantitative RT-PCR (qRT-PCR)

Total RNA was extracted with RNeasy Plant Mini Kit (Qiagen) using 70 mg of cryogenically-ground leaf and treated with DNAse (Roche Diagnostics). RNA purity was assessed by the 260/280 nm ratio, quantified with Nanodrop (Thermo Scientific) and integrity checked by electrophoresis. Reverse transcription was performed with Transcriptor First Strand cDNA Synthesis Kit (Roche Diagnostics). Each qRT-PCR reaction was performed in duplicate with GoTaq® qPCR Master Mix reagents in a volume of 20 µl, using StepOnePlus Real-Time PCR System (Thermo Scientific). Reaction parameters consisted in 95°C for 10 min, followed by 40 cycles at 95°C for 15 s and 60°C for 1 min. Primers for three stable reference genes (CAC, EF1-α, PGK) and for genes of interest were retrieved from literature or designed with Vector NTI Advance 10 software (Invitrogen) (Table 3.1). The results were expressed into fold change using the formula described (Hellemans et al., 2007) which takes into account three reference genes by a geometrical averaging using the mean of threshold cycle value obtained on the control plants as calibrator and analyzed with ANOVA ($P < 0.05$).

Table 3.1: List of genes studied.
SGN unigene ID from Sol Genomics Network and corresponding primers used for qRT-PCR.

Gene	Function	Accession	Primer sequences (5'-3')	References
CAC	Clathrin adaptor	SGN-U566667	CCTCCGTTGTGATGTAACTGG ATTGGTGGAAAGTAACATCATCG	Exposito-Rodriguez *et al.* (2008)
EF1-a	Elongation factor 1-α	SGN-U580418	CCAGATTGGAAACGGATATGC TCCTTACCTGAACGCCTGTCA	Nicot *et al.* (2005)
PGK	Phosphoglycerate kinase	SGN-U578082	TCTACAAGGCCCAAGGTTATG GCAGCAAACTTGTCCGCAATC	Ghareeb *et al.* (2011)
PR1	PR protein 1	SGN-U579545	TGTCCGAGAGGCCAAGCTATAAC AATGAACCACCATCCGTTGTTGC	Song *et al.* (2011)
PR2a	Glucan endo-1,3-β-glucosidase A	SGN-U562796	AATCAAGATCTTGAAGCCCTAGCCA GATCAACTTCGTTTCCAACGGCTAT	This study
PR2b	Glucan endo-1,3-β-glucosidase B	SGN-U581016	GCACCTTTGCTCGTTAACATT TTGACGCGATCCATCTTGTA	This study
CHI 2;1	Chitinase, class II	SGN-U580857	TGCCTTTTTGGCTCAAACTT CCAGGACTTCCTTGTTCCTG	This study
CHI3	Acidic 26 kDa endochitinase	SGN-U581507	ACGCCATCCCCTAAAGATAC CTGCAGTATTTGGACCCATC	This study
CHI9	Basic 30 kDa endochitinase	SGN-U579551	TTCCTTGCCCAAACTTCC AGGAAACAGTAACCCCATGC	This study
P69b	Subtilisin-like protease b	SGN-U581430	TTATCACAGCAGTAAACACCGCCC CAGATTCTCCTTCAAATTCCTCTCCAT	This study
LoxD	Lipoxygenase	SGN-U569257	GACTGGTCCAAGTTCACGATCC ATGTGCTGCCAATATAAATGGTTCC	Fujimoto *et al.* (2011)
PI-1	Protease inhibitor I	SGN-U577558	GTGTACCAACAAAGCTTGCTAAAGA GTACAACAACACCCAAAATGTTGTC	Fujimoto *et al.* (2011)
NIM1	Non-inducible immunity 1	SGN-U585807	AATCGGCTTAGGGCTCTCTC TGCTTCTTCAGTTGACGCTCT	This study

2.8. Extraction and quantification of salicylic acid (SA)

Free SA extraction was performed on 0.5 g of cryogenically-ground leaf samples as previously described (Verberne *et al.*, 2002). SA separation was performed on Alltima C18-HL column (2.1 mm * 150 mm, 3 µm, Grace). The mobile phase was 0.2 M sodium acetate buffer pH 5.5/methanol (90/10). SA was detected with an Ultimate 3000 RS Fluorescence Detector (Dionex) with an excitation wavelength of 305 nm and an emission wavelength of 407 nm. Results were expressed in ng SA per g fresh weight and analyzed using ANOVA and SNK test for multiple comparisons ($P < 0.05$).

2.9. Greenhouse trial: powdery mildew on tomato leaves

A GEP greenhouse trial for the control of powdery mildew (*L. taurica*) under production conditions was conducted by "De Bredelaar B.V." (Elst, Netherlands). The powdery mildew susceptible tomato CV Capricia was grown on potting soil and the seedlings were transplanted on 22 May in a greenhouse. The trial was set up in a randomized block design with four repetitions of ten plants each. The experimental design included an untreated control, a chemical reference Imazalil at 100 g active ingredient (AI) per ha of leaf wall area (LWA), as previously defined (Pergher and Petris, 2008) and COS-OGA at 25 g AI per ha LWA. The test products and application schedule and volumes are detailed in Table 3.2. Sprayings were performed with about 14-day interval (A, C, E) for the chemical reference and with about 7-day interval (A-E) for the COS-OGA elicitor (Table 3.2) using a spray lance fitted with a whirl nozzle type TXA10VK at an operating pressure of 3 bars. The severity and incidence of powdery mildew were assessed on five randomly selected leaves on each of the ten plants per plot. Assessments starting on 17 June were performed weekly before each application and were continued until 21 days after the last application E (Table 3.2). Assessments of powdery mildew severity and incidence were analyzed with ANOVA, followed by Fisher's least significant difference (LSD) test for multiple comparisons ($P < 0.05$). The effects of the treatment on disease incidence and severity were converted into protection (%) following the Abbott formula (van Aubel *et al.*, 2014).

Table 3.2: Test products description and application sequence of the tomato trial carried out against powdery mildew (*L. taurica*) under greenhouse in the Netherlands. Applications were performed as follows: A on 10 June, B on 17 June, C on 22 June, D on 27 June, E on 4 July.

Product	AI content	Rate AI (ha LWA[a])$^{-1}$	Water volume l/(ha LWA)$^{-1}$	Rate AI (ha LWA)$^{-1}$	Application timing
Untreated control	-	-	-	-	-
COS-OGA[b]	12.5 g/l	2.0 l	500	25 g	A – B – C – D – E
Imazalil	100 g/l	1 l	500	100 g	A –C –E

[a] Leaf wall area (LWA) was defined by Pergher and Petris (2008) as LWA = 10 000 * b^{-1} * h with b, in m, being the row spacing and h, in m, being the height of the canopy.
[b] COS-OGA was provided by FytoFend SA in its commercial soluble liquid formulation, FytoSave® containing 12.5 g/L COS-OGA.

3. Results

The aim of this work was to study the intrinsic effect of the oligosaccharide complex COS-OGA. For all laboratory experiments, the control plants were therefore sprayed with the electrolytes solution (50 mM NaCl, 0.5 mM $CaCl_2$) necessary for inducing the so-called egg box conformation of OGAs, and with the adjuvant. The COS-OGA-treated plants were sprayed with the same solution to which 50 ppm of COS-OGA elicitor were added.

3.1. Peroxidase activity in tomato leaves

Peroxidases are involved in H_2O_2 production, a key early component of PTI. But beside ROS production, cell wall peroxidases also take part in phytoalexin synthesis, lignin and suberin formation and cross-linking of cell wall components, all pivotal processes for plant basal resistance (Almagro *et al.*, 2009; Daudi *et al.*, 2012; Francoz *et al.*, 2015). The activity of class III peroxidases was thus assayed in tomato leaves after COS-OGA or flg22 application performed one day before harvest (DBH). Both treatments showed a significant increase of peroxidase activity in comparison to their respective controls but the increase was higher for flg22 (Fig. 3.1). There was no significant difference between peroxidase activity in control plants sprayed with 50 mM NaCl, 0.5 mM $CaCl_2$, 0.1% Dehscofix and plants sprayed with 0.1% Tween 20. Flg22 is usually applied through syringe-infiltration but the present results show that tomato plants also perceive flg22 upon foliar spraying. For comparison, flg22 was applied at 5 ppm or 2.2 µM while COS-OGA at 50 ppm corresponds to a 35 µM concentration (EU Pesticide Database, 2015).

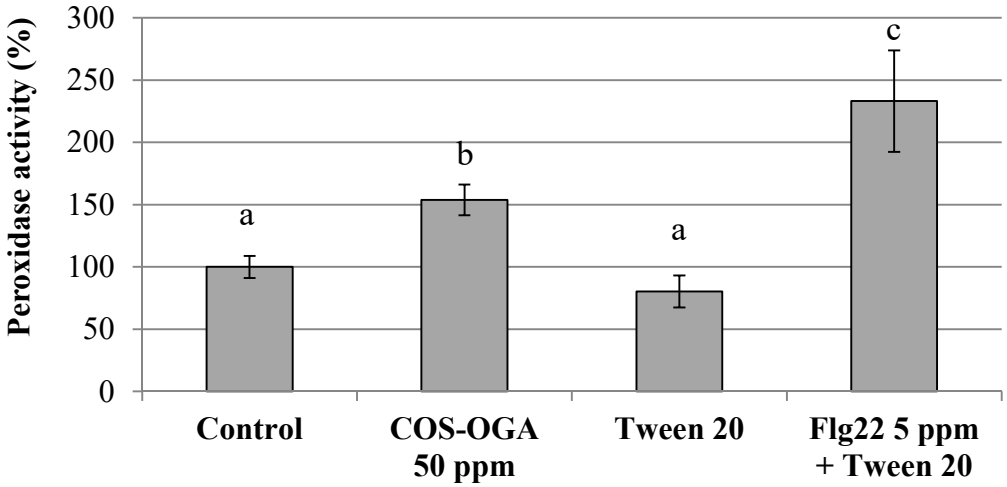

Fig. 3.1: Normalized peroxidase activity of tomato leaves CV Moneymaker sprayed one day before harvest (1 DBH). Results are expressed as mean ± standard deviation (n = 4) in percentage of the control (50 mM NaCl, 0.5 mM $CaCl_2$, 0.1% Dehscofix). Bars with different letters are statistically different (ANOVA and SNK test, $P < 0.05$).

In a second experiment peroxidase activity was assayed after one application of COS-OGA at one DBH or two applications at three and one DBH (Fig. 3.2). Leaf peroxidase activity increased more than 1.5-fold after one elicitor application and doubled after two applications, compared to control plants. The effect of COS-OGA on peroxidase activity was thus cumulative. The increase seen in control plants sprayed twice has probably to do with the mechanical stress caused by foliar spraying and not with the age of the plants since all plants were the same age. Water sprayed on leaves is indeed known to trigger the expression of defense-related genes, probably through mechanosensing (Braam and Davis, 1990).

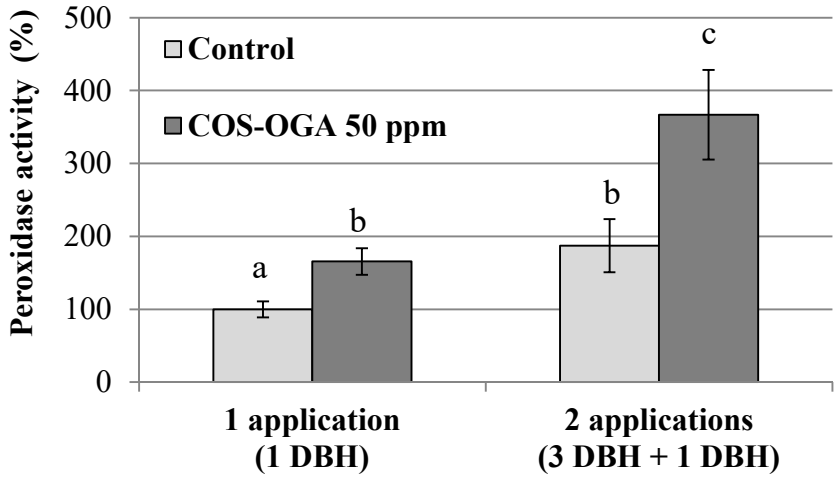

Fig. 3.2: Normalized peroxidase activity of tomato leaves CV Moneymaker sprayed one day before harvest (1 DBH) or twice at 3 DBH and 1 DBH. Results are expressed as mean ± standard deviation (n = 4) in percentage of the control (50 mM NaCl, 0.5 mM $CaCl_2$, 0.1% Dehscofix) sprayed at 1 DBH. Bars with different letters are statistically different (ANOVA and SNK test, $P < 0.05$).

3.2. Accumulation of defense-related proteins

A comparative 2D-DIGE proteomic analysis of tomato leaves was carried out to study the effect of repeated sprayings with COS-OGA at three and one DBH. Out of 1,661 protein spots that matched reproducibly between the different gels, 64 spots were significantly regulated ($P < 0.05$) by the elicitor with at least a 1.2-fold variation. Among them, 35 spots identified by MS contained one single protein. These regulated proteins were classified into several groups according to their main metabolic functions (Table 3.3). COS-OGA effect on proteome regulation appeared mainly positive as it globally increased the level of the differentially abundant proteins.

The most regulated group is the one of proteins involved in defense and stress response which mainly contains PR-proteins including a chitinase (CHI3), a β-1,3-glucanase (PR2a) and three subtilisin-like proteases (P69B, Table 3.3). PR proteins are mainly secreted in the apoplasm and in extracellular spaces and target pathogen cell walls that contain chitin, glucans and proteins (Edreva, 2005). Subtilisin-like protease P69B which is a specific serine endoproteases actively involved in plant defense, showed the highest increase in terms of abundance and was identified alone in three different spots. Tomato P69 subfamily contains at least six members of P69 subtilisin-like proteases (P69A, B, C, D, E, F). P69 subtilisin-like proteases are synthesized as precursor proteins containing both a signal peptide targeting the extracellular space and a propeptide that needs to be cleaved to activate the potentially glycosylated enzyme (Figueiredo *et al.*, 2014; Meichtry *et al.*, 1999). This could explain why P69 subtilisins appeared to be clustered in the same region of the gel and that P69B was also found in two other spots but in combination with other proteins.

COS-OGA induced the accumulation of cinnamoyl CoA reductase-like protein and polyphenol oxidase (Table 3.3), both involved in lignin synthesis for mechanically strengthening plant cell walls against pathogens. Cinnamoyl CoA reductase-like also known as PAR2 because of a phenylacetaldehyde reductase activity, uses products from the phenylpropanoid pathway to form monolignols, the building blocks of lignin polymers (Pan *et al.*, 2014). The polyphenol oxidase (PPO) catalyzes the oxidation of phenolic compounds to quinones and seems to take part in radical coupling of monolignols and in ROS generation (Mayer, 2006; Sullivan, 2015). COS-OGA also induced the accumulation of multicystatin, a cysteine protease inhibitor which acts as a defense protein by inhibiting cysteine proteases in insect guts but also regulates endogenous plant proteinases (Benchabane *et al.*, 2010).

Both polyphenol oxidase and cystatin are induced by the octadecanoid wound-signaling pathway polyphenol oxidase and cystatin are induced by the octadecanoid wound-signaling pathway (Koussevitzky *et al.*, 2004). Tomato spraying with COS-OGA increased the abundance of annexin p34 (AN34, Table 3.3). Annexins are mainly regulated by Ca^{2+} and possess activities including actin binding, phosphodiesterase activity, peroxidase activity and phospholipids binding. Transcripts coding for AN34 accumulate in tomato plants after treatment with gibberellic acid and ethephon or upon several abiotic stresses (Lu *et al.*, 2012). The abundance of HSR203, a CXE carboxylesterase with a serine hydrolase activity was also significantly increased by COS-OGA (Table 3.3). Interestingly, a concomitant increase in transcription and activity levels of HSR203 and P69B is observed just before the hypersensitive response (HR) in tomato leaves (Sueldo *et al.*, 2014).

The second class of proteins regulated by COS-OGA is involved in protein synthesis and folding. This class contains mainly positively regulated molecular chaperones among which two members of the HSP70 family (BIP5 and HSC-2), a chaperone protein HtpG (Table 3.3) bearing a conserved domain from the HSP 90 family and the gamma subunit of the T-complex protein 1 (Table 3.3). The accumulation of HSP is correlated with resistance to stress. Beside protein folding, HSP 90 family members also play a key role in cellular signal regulation and seem to be necessary for functionality of PRR. (Al-Whaibi, 2011; Caplan *et al.*, 2009). COS-OGA down-regulated two elongation factors (ELF2 and GUF1 homolog) that possess a reciprocal best BLAST hit (RBH) (Ward and Moreno-Hagelsieb, 2014) with two proteins involved in cold-induced translation in *Arabidopsis*, namely LOS1 for ELF2 and SVR3 for GUF1 homolog (Arisz *et al.*, 2013; Liu *et al.*, 2010).

The third class of proteins regulated by COS-OGA is linked to photosynthesis and energy metabolism (Table 3.3). Isocitrate dehydrogenase that produces NADH in the citric acid cycle was more abundant after treatment as well as NADP-dependent glyceraldehyde phosphate dehydrogenase subunit B which was recently shown to bind SA *in vitro* (Manohar *et al.*, 2015). Two chaperonins necessary for proper Rubisco subunits folding and assembly were also regulated: one putative rubisco subunit binding-protein and one Rubisco activase that restore enzyme activity by mediating the Rubisco conformational change required to release its substrate (Houtz and Portis Jr, 2003). Rubisco activase was also found in spot 1450 regulated 2.83 fold but in combination with trace of one other protein.

Table 3.3: List of identified proteins showing significant variation after treatment of tomato leaves with COS-OGA elicitor.

Spot n°[a]	SGN accession n°[b]	Protein	Theoretical pI/Mw (kDa)	Mascot score	Peptides matched[c]	Fold change[d]	t-test[e]
Defense and stress response							
312	Solyc00g071180.2.1	Cysteine proteinase inhibitor (multicystatin)	5.8/84.9	431.0	6	1.59	0.013
456	Solyc08g079870.1.1	Subtilisin-like protease B (P69B)	6.3/78.9	718.7	12	1.64	0.025
359	Solyc08g079870.1.1	Subtilisin-like protease B (P69B)	6.3/78.9	336.1	4	2.37	0.000
361	Solyc08g079870.1.1	Subtilisin-like protease B (P69B)	6.3/78.9	760.5	12	2.92	0.000
555	Solyc08g074630.1.1	Polyphenol oxidase (PPO)	6.0/66.3	446.9	8	1.44	0.039
1295	Solyc02g069800.1.1	CXE carboxylesterase (HSR203)	4.8/37.2	133.3	2	1.36	0.000
1426	Solyc01g008550.2.1	Cinnamoyl CoA reductase-like protein (PAR2)	6.0/35.4	206.1	5	1.36	0.005
1461	Solyc04g073990.2.1	Annexin p34 (AN34)	5.4/35.8	256.3	4	1.21	0.007
1449	Solyc01g008620.2.1	β-1,3-glucanase (PR2a)	6.6/37.5	125.0	3	2.19	0.002
1798	Solyc02g082920.2.1	Chitinase, class II (CHIT3)	5.9/27.6	192.0	3	1.7	0.002
Protein synthesis and folding							
196	Solyc08g062920.2.1	Elongation factor 2 (ELF2), GTP-binding	5.8/94.1	639.4	14	-1.24	0.008
221	Solyc04g081570.2.1	Chaperone protein htpG	4.9/93.3	392.8	7	1.25	0.008
348	Solyc03g058190.2.1	Elongation factor GUF1 homolog, GTP-binding	6.3/74.2	488.7	8	-1.21	0.029
416	Solyc03g082920.2.1	Heat shock protein 70-3 (BIP5)	5.1/73.4	1415.1	26	1.28	0.000
443	Solyc10g086410.2.1	Heat shock cognate 70 kDa protein 2 (HSC-2)	5.1/70.7	1256.3	26	1.21	0.002
530	Solyc05g056310.2.1	T-complex protein 1, subunit gamma	5.7/60.7	386.6	4	1.25	0.000
Photosynthesis and energy metabolism							
510	Solyc11g069790.1.1	Chaperonin Cpn60, RuBisCO large subunit-binding protein, chloroplastic	5.2/61.9	1034.2	16	-1.25	0.011
1094	Solyc01g005560.2.1	Isocitrate dehydrogenase, NADP-dependent	6.3/46.7	1027.1	21	1.29	0.001
1425	Solyc12g094640.1.1	Glyceraldehyde-3-phosphate dehydrogenase B	6.7/48.0	77.5	2	1.21	0.001
1743	Solyc10g086580.1.1	Ribulose-1 5-bisphosphate carboxylase/oxygenase activase 1	8.6/50.7	255.1	3	1.27	0.012
DNA/RNA remodeling							
310	Solyc08g042050.2.1	DEAD-box ATP-dependent RNA helicase 3 (SlDEAD25)	6.3/81.5	965.8	20	1.24	0.043
311	Solyc08g042050.2.1	DEAD-box ATP-dependent RNA helicase 3 (SlDEAD25)	6.3/81.5	620.4	9	1.39	0.010
1228	Solyc06g073260.2.1	NAD-dependent epimerase/dehydratase	7.7/42.4	131.3	2	1.35	0.004

Table 3.3: List of identified proteins showing significant variation after treatment of tomato leaves with COS-OGA elicitor.

Spot n°[a]	SGN accession n°[b]	Protein	Theoretical pI/Mw (kDa)	Mascot score	Peptides matched[c]	Fold change[d]	t-test[e]
pH homeostasis							
366	Solyc06g063330.2.1	V-type ATP synthase alpha chain, subunit A	5.2/68.5	114.2	2	1.21	0.001
931	Solyc01g007320.2.1	ATP synthase subunit beta, chloroplastic	5.3/53.4	436.2	9	1.25	0.000
1523	Solyc08g081910.2.1	V-type proton ATPase subunit E	6.3/26.4	433.0	8	1.25	0.014
Redox homeostasis							
599	Solyc06g005940.2.1	Protein disulfide isomerase	4.8/54.8	203.2	4	1.43	0.002
603	Solyc06g005940.2.1	Protein disulfide isomerase	4.8/54.8	629.3	15	1.49	0.000
1903	Solyc06g009020.2.1	Glutathione S-transferase (GST)	6.0/23.7	333.2	6	1.26	0.001
Carbon metabolism							
347	Solyc11g069380.1.1	4-hydroxy-3-methylbut-2-en-1-yl diphosphate synthase (HDS)	5.8/82.2	588.6	12	-1.25	0.022
1877	Solyc02g086820.2.1	Chloroplast carbonic anhydrase (CA2)	6.7/34.4	338.7	7	-1.24	0.014
Other							
241	Solyc09g031970.2.1	Glycogen/starch/alpha-glucan phosphorylase	6.2/94.9	557.6	17	1.79	0.000
270	Solyc07g006810.2.1	Adenosylmethionine-8-amino-7-oxononanoate aminotransferase-like protein	5.9/95.0	310.9	5	1.32	0.001
340	Solyc01g107130.2.1	Vacuolar sorting receptor	5.4/69.8	322.1	4	1.38	0.000
1433	Solyc06g068220.2.1	Hydrolase alpha/beta fold family protein, epoxide hydrolase-like	6.2/42.4	211.8	4	1.21	0.001

[a] Spot number corresponding with the 2-D gel as shown in Fig. S2 (Supplementary data, available online)

[b] Sol Genomics Network accession number

[c] Number of sequenced peptides exclusively assigned to the protein

[d] Protein fold change given by the standardized average ratio in spot quantity between the two groups (Student t test, $P < 0.05$). Positive and negative values indicate up- and down-regulation respectively by the COS-OGA elicitor treatment

DNA/RNA remodeling proteins were overexpressed following elicitation. The DEAD-box ATP-dependent RNA helicase 3 (SlDEAD25, Table 3.3) identified twice is a zinc finger protein that removes stress-induced secondary structures in mRNA and interacts with topoisomerases to modify gene expression or activate transcription factors to express stress-related genes (Vashisht and Tuteja, 2006). DEAD-box helicases are regulated at posttranslational levels notably by phosphorylation (Gustafson and Wessel, 2010) which probably explains why SlDEAD25 was found in two different spots with similar molecular weight but different pI. In rice, SA treatment induces overexpression of a DEAD-box RNA helicase OsBIRH1. OsBIRH1-overexpressing transgenic *Arabidopsis* showed an enhanced disease resistance coupled to an increased expression of PR1, PR2, and ascorbate peroxidase genes (Li *et al.*, 2008). COS-OGA also induced the accumulation of a NAD-dependent epimerase/dehydratase (Table 3.3) that shows a RBH with the Arabidopsis protein CSP41B that binds and stabilizes chloroplast mRNA (Baker *et al.*, 1998; Qi *et al.*, 2012) in a redox state-dependent manner and seems involved in heat and salinity stress tolerance by improving photosynthesis (Ariga *et al.*, 2015).

Three proteins involved in pH homeostasis were upregulated by COS-OGA: a vacuolar ATP synthase (V-type), a chloroplastic ATP synthase and a vacuolar ATPase (Table 3.3). These enzymes involved in transport coupled to ATP hydrolysis take part in pathogen signal regulation by mediating a cytoplasmic pH shift (Elmore and Coaker, 2011).

Proteins involved in redox homeostasis were also upregulated after elicitation. A protein disulfide isomerase (Table 3.3) which is a redox–sensitive molecular chaperone that catalyzes cysteine disulfide bonds formation was identified twice in two close spots. In *Arabidopsis*, a protein disulfide isomerase has been identified among early responsive proteins that accumulate and undergo cysteine oxidative modification in response to treatment with salicylate or with flg22 (Liu *et al.*, 2015b). COS-OGA treatment also induced the accumulation of a glutathione S-transferase (GST, Table 3.3) known to use glutathione mainly for detoxification of xenobiotics and toxic lipid peroxides. In tomato, GST is associated with the reduction of oxidative damage, SA treatment and salt stress (Csiszár *et al.*, 2014).

Two chloroplast proteins involved in the carbon metabolism were less abundant after elicitor treatment: the carbonic anhydrase (CA2, Table 3.3) and the 1-hydroxy-2-methyl-2-butenyl 4-diphosphate synthase (HDS, Table 3.3). Carbonic anhydrase catalyzes the reversible hydration of carbon dioxide and HDS is implicated in the methylerythritol phosphate pathway leading to isoprenoid biosynthesis and functions as a stress sensor. The repression of HDS induces the accumulation of its substrate methylerythritol cyclodiphosphate (MEcDP) which is a stress-specific organelle to nucleus retrograde signal (Xiao *et al.*, 2012). In C3 plants like tomato, carbonic anhydrases from the beta type like CA2 take part in the optimization of CO_2 availability to Rubisco, as well as in the CO_2 signaling pathway that controls stomatal movements (Hu *et al.*, 2010). MAMP-triggered stomatal closure is an important factor of PTI that requires SA (Zeng *et al.*, 2010) and the *Arabidopsis* SA-binding protein 3 (SABP3) has recently been identified as a chloroplastic carbonic anhydrase involved in HR (Manohar *et al.*, 2015).

The remaining proteins upregulated by COS-OGA were grouped in the class “other” involving less-represented metabolic processes: a glycogen/starch alpha-glucan phosphorylase, an adenosylmethionine-8-amino-7-oxononanoate aminotransferase-like, a vacuolar sorting receptor and a hydrolase alpha/beta fold family. The glycogen/starch alpha-glucan phosphorylase converts starch or glycogen into glucose-6-phosphate: a higher hexose phosphate availability allows the plant to quickly respond to environmental modifications (Zeeman *et al.*, 2004). The protein adenosylmethionine-8-amino-7-oxononanoate aminotransferase-like is involved in biotin metabolism. Biotin is an important coenzyme for carboxylases but it is also involved in regulation of gene expression through chromatin remodeling by histone biotinylation (Li *et al.*, 2012). The vacuolar sorting receptor identified here possesses a RBH with ATVSR3 in *Arabidopsis* which is specifically expressed in guard cells and seems involved in stomatal closing mediated by ABA (Avila *et al.*, 2008).

3.3. Expression of SA-related genes and PR proteins

The three housekeeping genes CAC, EF1-α and PGK proved to be stable in our experimental conditions (Fig. 3.3). *PR1* and *PR2b* encoding the PR1 protein and the glucan endo-1,3-beta-glucosidase A (Song *et al.*, 2011), both SA-responding genes, were strongly upregulated after COS-OGA treatments. The expression of both *LoxD* encoding a 13-lipoxygenase involved in JA pathway (Finiti *et al.*, 2014) and *PI-1* encoding the protease inhibitor 1 linked to JA and ET (Fujimoto *et al.*, 2011) remained constant.

CHI2;1 and *CHI9* encoding a class II and a class I chitinase respectively were also overexpressed after COS-OGA treatments. *CHI2;1* is a PR gene associated to ET signaling (Balaji *et al.*, 2008) while transcripts of *CHI9* accumulate in tomato leaves following spraying with ET and methyl jasmonate, but not with SA (Wu and Bradford, 2003). *NIM1*, the *NPR1* orthologue in *Solanaceae*, showed no significant increase following COS-OGA treatments. SA perception relies on the SA receptors NPR1 and its paralogs, NPR3 and NPR4 but a higher expression of NIM1 is not necessarily required for SAR induction and studies on SA over-accumulating mutants reveal that even if NPR1 seems to be the major route of response to SA, some SA-dependent signaling pathways are NPR1-independent (Janda and Ruelland, 2015).

We also designed specific primers for the *PR2a*, *CHI3* and *P69B* genes that code for proteins known to be mainly associated with the SA pathway and that were more abundant in our 2D-DIGE study after COS-OGA treatment. qRT-PCR results were consistent with the 2D-DIGE as *PR2a*, *CHI3* and *P69B* transcripts were also significantly upregulated (Fig. 3.3).

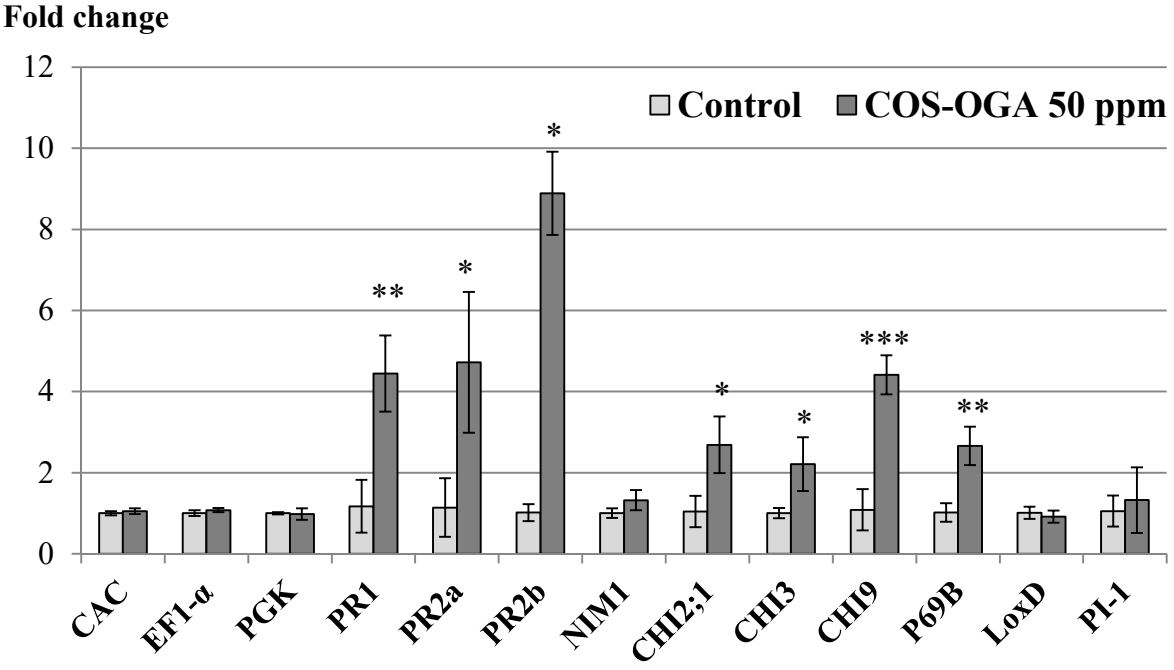

Fig. 3.3: Variation in genes expression quantified by qRT-PCR on tomato leaves CV Moneymaker. Tomato plants were sprayed one and three days before harvest. Results are presented as mean ± SD (n = 4). Bars with asterisk are considered as differently expressed (ANOVA with * for $P < 0.05$, ** for $P < 0.01$, *** for $P < 0.001$).

3.4. Free SA accumulation in leaves

Free SA was measured in leaves after one (1 DBH), two (3 and 1 DBH) or three applications (7, 3 and 1 DBH) of COS-OGA. Free SA accumulated in leaves starting with the second application and it seemed to be a function of the number of sprayings (Fig. 3.4). The ANOVA test showed indeed a highly significant effect of the number of sprayings on SA level for COS-OGA treatment (P = 0.001). SA accumulation had already been observed in tomato seedlings following application of other SAR-inducing oligosaccharides from algal origin (El Modafar *et al.*, 2012) but to our knowledge it is the first time that a cumulative effect of the number of elicitor applications on SA content is demonstrated.

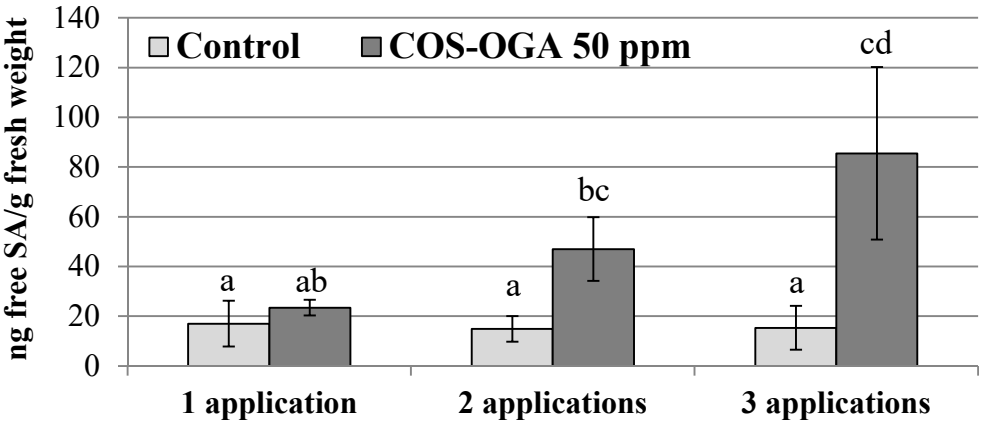

Fig. 3.4: Free salicylic acid (SA) content of tomato leaves CV Moneymaker. Tomato plants were sprayed once at 1 DBH, twice at 3 and 1 DBH or three times at 7, 3 and 1 DBH. Results were expressed as mean ± SD (n = 4). Bars with different letters are statistically different (ANOVA and SNK test, $P < 0.05$).

3.5. Powdery mildew severity on tomato leaves

The severity of powdery mildew development on tomato leaves following natural contamination in greenhouse is presented in Fig. 3.5. The disease was already present at a very low level at the first evaluation of the trial on 17 June. On July 4, the severity increased dramatically in untreated controls. Between 4 July and 11 July, the severity was significantly lower in COS-OGA treated plants as well as in the chemical reference (Imazalil). On 18 and 25 July, two and three weeks respectively after the last treatment, COS-OGA still reduced significantly the disease severity compared to control plants. Powdery mildew incidence (Fig. 3.6) was already high in untreated control plants at the beginning of the trial with 44% of plants affected and it increased slightly up to 50% at the end of the trial. COS-OGA and Imazalil significantly reduced disease incidence before the last observation on 25 July when

treatments were not any more efficient. As already observed, COS-OGA has always a higher efficacy in terms of severity than incidence because it does not kill the pathogen but it mobilizes host defenses that limit the spread of the disease (van Aubel *et al.*, 2014). This is why the protection in terms of severity obtained by spraying with COS-OGA reached 90% on 11 July while for disease incidence, the protection decreased down to 40% on 18 July before disappearing at the last evaluation.

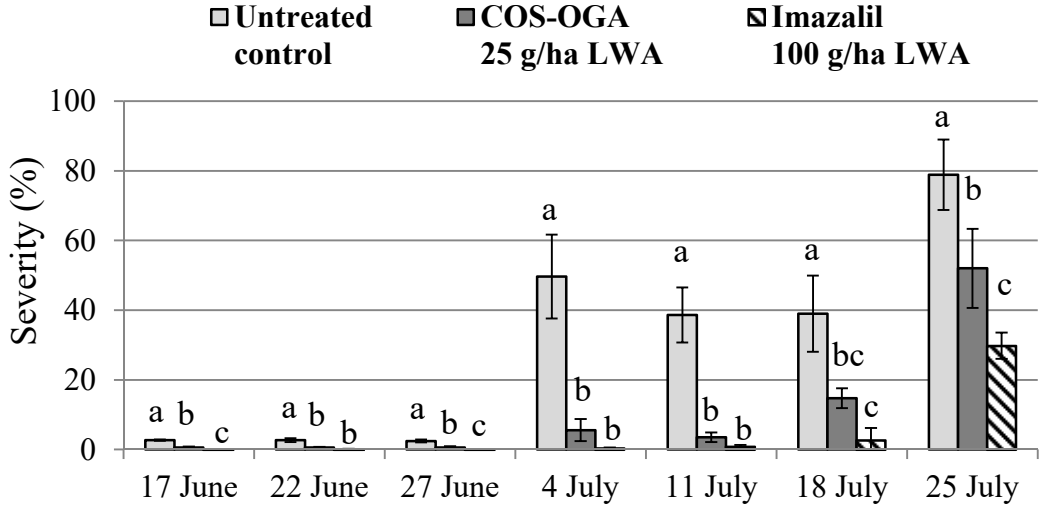

Fig. 3.5: Mean (± SD) of powdery mildew severity on tomato leaves CV Capricia. Tomato plants were sprayed with 500 l (ha LWA)$^{-1}$ either five times with 2 l (ha LWA)$^{-1}$ of a liquid formulation containing 12.5 g/l COS-OGA or three times with 1 l (ha LWA)$^{-1}$ of the chemical reference, a liquid formulation containing 100 g/l Imazalil. Values with different letters are significantly different for each individual date of evaluation (ANOVA and Fisher LSD test, P <0.05).

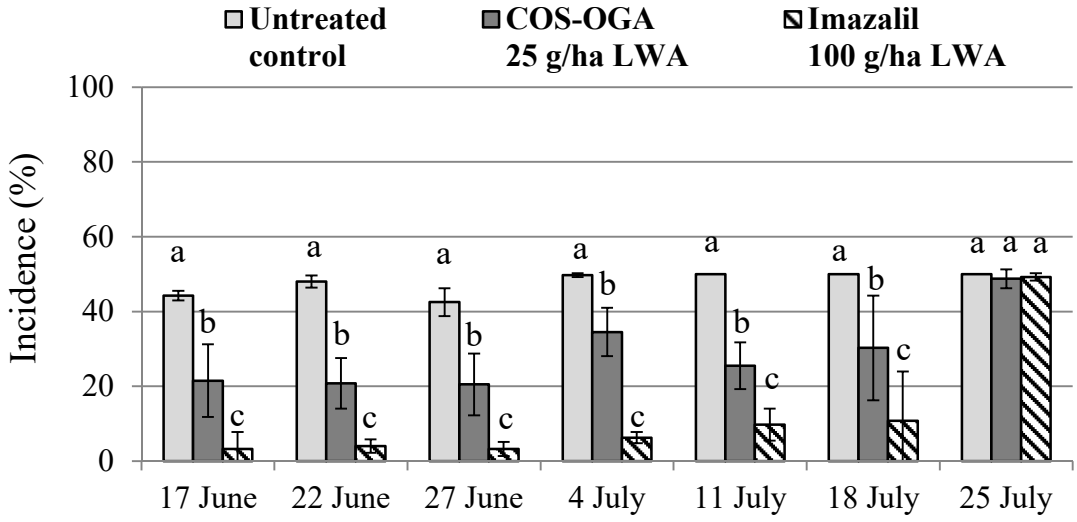

Fig. 3.6: Mean (± SD) of powdery mildew incidence on tomato leaves CV Capricia.
Plants were sprayed either five times with 2 l (ha LWA)$^{-1}$ of a liquid formulation containing 12.5 g/l COS-OGA or three times with 1 l (ha LWA)$^{-1}$ of a liquid formulation containing 100 g/l Imazalil, in a total water volume of 500 l/ha LWA. Values with different letters are significantly different for each individual date of evaluation (ANOVA and Fisher LSD test, P <0.05).

4. Discussion

The mode of action of COS-OGA, a new oligosaccharide elicitor, was investigated on tomato plants. Control and elicited plants were analyzed with 2D-DIGE and mass spectrometry for soluble protein changes. Transcription of specific genes known to be involved in SA and JA signaling pathways was also tested by RT-qPCR. Since all results pointed toward a stimulation of SA-related defenses, SA was assayed in control compared to treated plants. Finally, the protection of tomato conferred by COS-OGA was tested in greenhouse against *L. taurica*, a powdery mildew agent.

The leaf proteomic study revealed that in absence of pathogen, COS-OGA induced accumulation of SA-related PR proteins. Among those proteins, the levels of the P69 subfamily of subtilisin-like proteases were particularly increased. It is known that exogenous SA application induces the expression of *P69B* and *P69C* genes in tomato (Jorda and Vera, 2000). But P69C seems to operate upstream of the SA pathway as the expression of *SBT3.3*, the *Arabidopsis* orthologue of tomato subtilisin *P69C*, is NPR1-independent, is increased by H_2O_2 application and is required for downstream expression of SA-responsive genes. Congruently, the P69 subfamily of subtilisin-like proteases is suspected to be an activator of PTI by processing an ectodomain of a membrane receptor, thereby triggering an intracellular signaling pathway (Ramírez *et al.*, 2013). Earlier transcription of subtilisin-like protein is also observed in resistant grapevine CV after downy mildew inoculation comparatively to sensitive CV (Monteiro *et al.*, 2013). Subtilisin accumulation following COS-OGA spraying could thus indicate a SA-dependent mode of action involving PRR activation.

It is well known that the apoplastic class III peroxidase-generated oxidative burst plays an essential role in PTI triggered by pathogen attack [6]. Peroxidases are largely present among proteins regulated by exogenous SA application (Hao *et al.*, 2012) but they were not identified by 2D-DIGE among the leaf proteins regulated by COS-OGA, despite a significant increase in leaf peroxidase activity after treatment. The buffer we used for testing peroxidase activity *in vitro* contained a large amount of NaCl to release cell wall-bound class III peroxidases while our 2D-DIGE was directly performed on total soluble protein extracts. An additional step of cell wall fractionation followed by concentrated NaCl treatment prior to TCA/acetone precipitation should be carried out to retrieve class III peroxidases accumulated following tomato spraying with COS-OGA in 2D-DIGE (Tiffany Paques, unpublished results).

Extracellular ROS are a key early component of PTI and originate from both membrane NAPDH oxidases (RBOH) and cell wall peroxidases (Wrzaczek *et al.*, 2013). ROS origin seems to determine its biological activity as there are indications in *Arabidopsis* that ROS produced by RBOHD suppress the spread of cell death mediated by SA and that RBOHD and RBOHF are essential for expression of JA-induced genes (Maruta *et al.*, 2011). Peroxidases appear to be a major producer of H_2O_2 during plant defense beside NADPH oxidases: in *A. thaliana* cell suspensions, H_2O_2 production due to COS-OGA treatment is mainly apoplastic and originates from peroxidases [62]. Here, COS-OGA considerably increased guaiacol peroxidase activity in leaves and the resulting production of H_2O_2 could have activated transcription of subtilisin-like proteases, as discussed above. The guaiacol peroxidase activity induced by the powdery mildew agent *Oidium neolycopersici* has been shown to be higher in semi-resistant tomato CVs than in a susceptible one and is correlated with H_2O_2 production and the expression of HR (Tománková *et al.*, 2006). COS-OGA also induced the accumulation of HSR203 and P69B proteins, both serine hydrolases whose transcripts levels and enzymatic activities were shown to specifically increase in tomato just before HR: *Hsr203* transcripts accumulation is considered as a marker of HR activation in several species (Sueldo *et al.*, 2014).

Plant response to COS-OGA also likely involves epigenetic control, considering the increase in subtilisin-like proteases, chaperones, HSP and DNA/RNA remodeling enzymes after treatment. Indeed, the overexpression of *SBT3.3* in *Arabidopsis* promotes chromatin remodeling, resulting in faster and stronger SA-dependent defense (Ramírez *et al.*, 2013). COS-OGA spraying also induced the accumulation of a NAD-dependent epimerase/dehydratase and a DEAD-box ATP-dependent RNA helicase, respectively involved in stabilization of chloroplast mRNA and unwinding of RNA before translation. COS-OGA seems thus to act both on transcriptional and translational mechanisms and this epigenetic regulation could be the hallmark of priming by this elicitor.

The accumulation of PR proteins observed in 2D-DIGE was in agreement with qRT-PCR results obtained for *PR2a*, *CHI3* and *P69B* as well as for the SAR marker, PR1. Although PR proteins are not always linked to one specific pathway *per se*, the overexpression of PR1 clearly points to SAR stimulation, which was confirmed by assaying free SA accumulation following COS-OGA application. We can thus assume that COS-OGA stimulates the SA pathway, but without excluding involvement of JA and ET as some genes that respond to these plant hormones also reacted to COS-OGA application.

However, transcripts specific to ISR and linked to JA and ET like *LoxD* and *PI-1* (Finiti *et al.*, 2014; Fujimoto *et al.*, 2011; van Loon *et al.*, 2006b) were not regulated.

Beta-glucosidases (PR2a, PR2b) and P69 subtilisin-like protease are often linked to the SA pathway and chitinases (PR3 or CHI3 and CHI9) to the JA pathway (Ahmad *et al.*, 2014), while Wu and Bradford (2003) report that foliar expression of *CHI9 and PR2a* is strongly upregulated by ET and methyl jasmonate but not by SA. However, the accumulation of several chitinases in leaves of cucumber plants grown on Hoagland solution supplemented with 0.05 mM SA is also described by Hao *et al.* (Hao *et al.*, 2012). His results are similar to ours for several groups of proteins, especially those linked with photosynthesis and energy metabolism and with protein synthesis and folding. We also observed an increase in Rubisco activase, an enzyme that maintains Rubisco in an active conformation, thereby contributing to increased carbon fixation. Next to Rubisco activase, several enzymes of the Calvin cycle were also increased by COS-OGA, which is consistent with the absence of metabolic cost associated with the use of the elicitor (van Aubel *et al.*, 2014). However, a striking difference is that CA2 and HDS, two proteins involved in carbon metabolism, are overexpressed after SA treatment (Hao *et al.*, 2012) but down-regulated by COS-OGA. Interestingly, the *Arabidopsis* mutant *csb3 (constitutive subtilisin 3*) that overexpresses the *SBT3.3* gene encoding the orthologue of tomato P69C was shown to be impaired in HDS activity. *csb3* is more resistant to *P. syringae* DC3000 and *Hyaloperonospora arabidopsis*, accumulates SA and has a higher expression of the SA-inducible genes *PR1*, *PR2* and *GST6* (Gil *et al.*, 2005). Here, we also observed after COS-OGA treatment, an accumulation of SA, an overexpression of *PR1* and *PR2* genes, an accumulation of subtilisin-like proteases and a decrease in HDS and GST levels. Moreover, the GST that increased in our study is the homolog of the GST6 accumulated in the *csb3* mutant. In this mutant, accumulation of MEcDP, the HDS substrate that seems to stimulate genes linked to the SA and JA pathways, also induces the expression of two nuclear-encoded plastidial proteins, isochorismate synthase that takes part in SA synthesis and hydroperoxide lyase involved in oxylipins pathway (Gil *et al.*, 2005). COS-OGA seems to partly mimic the effect of the *csb3* mutation and it will be interesting to see if the induction of SA-dependent plant defense by COS-OGA is also linked with MEcDP accumulation.

Although plants prioritize the SA pathway after COS-OGA application, one cannot exclude involvement of other hormones since proteins known to respond to JA and ET were also regulated by COS-OGA. SA and JA antagonism is in fact dose-dependent and synergy between the two hormones can appear especially at low concentrations (Mur *et al.*, 2006). Rhamnolipids application on *Arabidopsis* involves several hormonal signaling pathways in response to pathogen challenge, depending on the type of pathogen feeding strategy: rhamnolipids-induced resistance requires both SA and ET signaling in presence of the hemibiotrophic bacterium *P. syringae* and the biotrophic oomycete *Hyaloperonospora arabidopsis*, while SA and JA signaling is activated in presence of the necrotrophic fungus *Botrytis cinerea* (Sanchez *et al.*, 2012). The type of pathogen influences the defense pathways induced and it will be interesting to see how plant defenses are mobilized by COS-OGA in presence of pathogens with different feeding strategies.

Microarray studies performed either on *Brassica napus* treated with COS or on *A. thaliana* cell suspensions treated with OGA both show a strong regulation of genes involved in JA and ET signaling (Moscatiello *et al.*, 2006; Yin *et al.*, 2006). Here the combined COS and OGA mainly acted on SA-regulated genes, indicating that the two oligosaccharides work synergistically in the COS-OGA complex. Wall-associated kinase 1 is a PRR candidate for binding of OGA in egg box conformation in *Arabidopsis* (Brutus *et al.*, 2010; Decreux and Messiaen, 2005) but no receptor has ever been characterized for COS, even if receptors have been identified for oligochitin (N-acetylglucosamine) perception (Boller and Felix, 2009). It remains to be studied if COS and OGA are perceived separately or as a complex by one or several PRRs. Beside a direct interaction with PRRs, the oligosaccharide complex could also interact with cell wall pectin, thereby indirectly activating wall integrity sensors (Wolf *et al.*, 2012).

In conclusion, results from proteomics, transcriptomics and SA quantification performed on tomato plants sprayed with COS-OGA all point toward a stimulation of SA-related defenses. This is consistent with the observed protection of tomato conferred by COS-OGA against powdery mildew provoked by a biotrophic plant pathogen. The key to elicitor efficacy in the present trial against powdery mildew probably resides in several cadenced sprayings. Indeed, the defense mechanism seems to be a cumulative process that includes peroxidase activation and free SA accumulation. Several applications of COS-OGA are probably necessary to increase the stimulation of plant defenses up to a threshold that allows efficient protection. Plant response to COS-OGA also likely relies on epigenetic control, considering the increase in subtilisin-like proteases, chaperones, HSP and DNA/RNA remodeling enzymes. In particular, the P69 subfamily currently sparks growing interest for its multiple roles in PTI including involvement in HR, immune memory, immune response modulation and putative receptor activation (Ramírez *et al.*, 2013).

5. Acknowledgments

This work was financially supported by the Service Public de Wallonie, Belgium (research grant No. D31-1302). We thank Bertrand Colignon, Edouard Delaive, Catherine Demazy and Caroline Thunissen for excellent technical assistance in the experiments.